

Experimental studies on CHF enhancement in pool boiling with CuO-water nanofluid

Ramakrishna N. Hegde · Shrikantha S. Rao ·
R. P. Reddy

Received: 21 September 2010 / Accepted: 22 December 2011 / Published online: 3 January 2012
© Springer-Verlag 2011

Abstract Critical heat flux enhancement (CHF) in pool boiling with CuO nanofluids was experimentally studied using a 36 gauge NiCr wire at atmospheric pressure. Experimentation included (1) subjecting the wire surface to multiple heating cycles with constant volume concentration of CuO nanofluid and (2) subjecting the wire surface to a single heating cycle with different volume concentrations of CuO nanofluid. Boiling of nanofluid in both the cases resulted in nanoparticle deposition and subsequent smoothing of the wire surface. To substantiate the nanoparticle deposition and its effect on critical heat flux, investigation was done by studying the surface roughness and SEM images of the wire surface. The experimental results show the evidence of nanoparticle deposition on the wire surface and its effect on CHF enhancement.

List of symbols

A Surface area (m^2)
C_p Specific heat (J/kg K)
D Diameter (m)

R. N. Hegde
National Institute of Technology, Surathkal, India

R. N. Hegde (✉)
Department of Mechanical Engineering, M. S. Ramaiah Institute of Technology, MSR Nagar, Bangalore 560054, India
e-mail: rkhegderk@gmail.com

S. S. Rao
Department of Mechanical Engineering, National Institute of Technology, Surathkal 575025, India
e-mail: ssrcsr@gmail.com

R. P. Reddy
Reva Institute of Technology,
Yelahanka, Bangalore 560064, India
e-mail: principalritm@revainstitute.org

g Gravitational acceleration (ms^{-2})
h_{fg} Latent heat of vaporization (J kg^{-1})
I Current (A)
k Thermal conductivity ($\text{Wm}^{-1}\text{K}^{-1}$)
L Length (m)
q Heat flux ($\text{Wm}^{-2}\text{K}^{-1}$)
U Uncertainty
V Voltage (V)
W Watt (W)

Greek symbols

ϕ Volume fraction
 ρ Density (kgm^{-3})
 σ Surface tension (Nm^{-1})
 μ Kinematic viscosity (m^2s^{-1})
 η Dynamic viscosity (Nm^{-2}s)

Subscripts

c Critical
CHF Critical heat flux
nf Nano fluid
m Mass
max Maximum
s Nano particle
l Liquid
v Vapour, volume

1 Introduction

With rapid advancement in the field of nuclear and fossil energy, electronic chips, electric power generation, compact computing devices etc., tremendous impetus is given to study the heat transfer phenomenon. Of late, heat transfer associated with phase change has gained lot of attention by engineers and researchers throughout the

world aimed at improving the heat transfer performance. The high rate of heat transfer results from the cooling liquid undergoing a phase change absorbing heat from a solid surface exposed to it. This rapid heat transfer is possible due to removal of heat from the surface as a combined effect of heat of vaporization and sensible heat, and motion of bubbles leading to rapid mixing of the fluid. This phenomenon of boiling heat transfer plays a crucial role in the design of high heat flux systems like boilers, heat exchangers, microscopic heat transfer devices, thermal ink jet printers etc. However, boiling phenomenon is limited by “boiling crisis” or critical heat flux (CHF) signifying the departure from nucleate boiling. At CHF, the material of the heated surface suffers physical damage due to inefficient or lower heat transfer resulting from a thin film formed over the surface. This has forced the researchers to focus on materials with enhanced thermal properties. With the surge of nanofluids as potential candidates for cooling fluids, many studies have been reported on enhancement of CHF and thermal conductivity using nanofluids.

Some of the studies on phase-changing heat transfer of nanofluids reported in recent times mainly focused on pool boiling heat transfer at atmospheric pressure that are briefed here in as follows.

Based on their experimental study on the CHF of water–Al₂O₃ nanoparticles-suspensions in a pool boiling experiment at the pressure of 20.89 kPa, You et al. [1] demonstrated that the CHF increased about 200% compared with pure water without any change in the nucleate boiling heat transfer coefficient.

Das et al. [2] conducted an investigation on the pool boiling of water–Al₂O₃ nanoparticles-suspension on a horizontal tubular heater of 20 mm diameter with different surface roughness at atmospheric pressure without using any surfactant into the fluid suspensions. They observed deterioration of the boiling heat transfer of nanoparticle compared to that of pure water. They further reported increase in wall superheat for nanofluids by about 30–130% with a volume concentration of 4% for pure water. They reasoned surface roughness of the heating surface affecting the nucleation superheat, as the required superheat for a smooth surface was higher than that for a rough surface.

Vassallo et al. [3] carried out a pool experiment of silica–water nanoparticles-suspensions on a horizontal NiCr wire at atmospheric pressure without using any surfactants. They reported CHF enhancement to the extent of 60% for horizontal wire surface in the pool. They found no appreciable differences in the boiling heat transfer for the heat flux below the CHF. The 50 nm silica solution used by them could give a maximum heat flux 3 times than that of pure water.

Bang and Chang [4] made an experimental investigation on the pool boiling of water–Al₂O₃ nanoparticle-suspensions on a plain plate at atmospheric pressure without using any surfactant. They reported degradation in nucleate boiling heat transfer characteristics when compared with that of pure water. For the horizontal test surface, however, the CHF of the nanofluid increased 32%. These were related to the change of the heating surface characteristics by the deposition of nanoparticles on the heating surface.

Wen [5] investigated the role of structural disjoining pressure arising from the confinement of nanoparticles in a meniscus in CHF enhancement. He showed that structural disjoining pressure can significantly increase the wettability of the fluids and inhibit dry patch development.

Kwark et al. [6] studied pool boiling behavior of low concentration nanofluids (≤ 1 g/l) experimentally over a flat heater at 1 atmosphere. They guessed boiling of nanoparticles produce a thin film on the heater surface is responsible for increase in CHF. Their study also indicated nanoparticle deposition results in transient characteristics in the nucleate boiling heat transfer. Further investigation by them revealed micro layer evaporation during nanofluid boiling was responsible for the formation of nanoparticle coating on the heater surfaces.

CHF prediction was first addressed by Kutateladze [7] to study saturated pool boiling and in the later stage Zuber [8] made an attempt to determine the CHF proposing the following relation.

$$\frac{q_c}{h_{fg}\rho_v^{0.5}[\sigma g(\rho_l - \rho_v)]^{\frac{1}{4}}} = 0.131 \quad (1)$$

As discussed above, over the last one decade only few analytical and experimental investigations on CHF enhancement in pool boiling using nanofluids have been done, some of those claiming contradictory results. In this context, to establish a reliable data it is very much essential to verify the claims made by researchers experimentally and analytically. With a similar intention experiments are conducted to verify the effect of surface roughness in CHF enhancement using CuO nanofluids.

2 Pool boiling experiment

2.1 Preparation and characterization of nanofluids

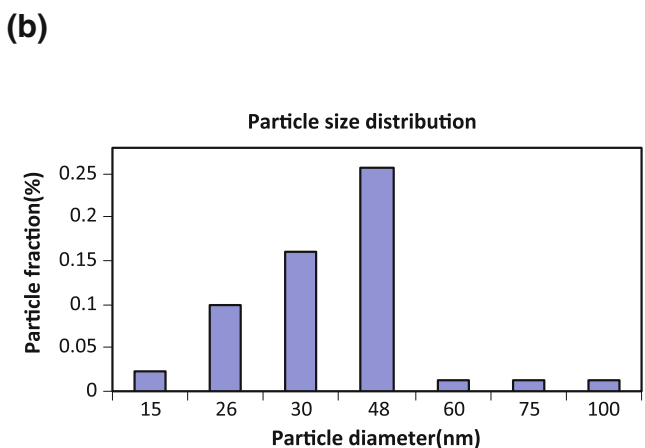
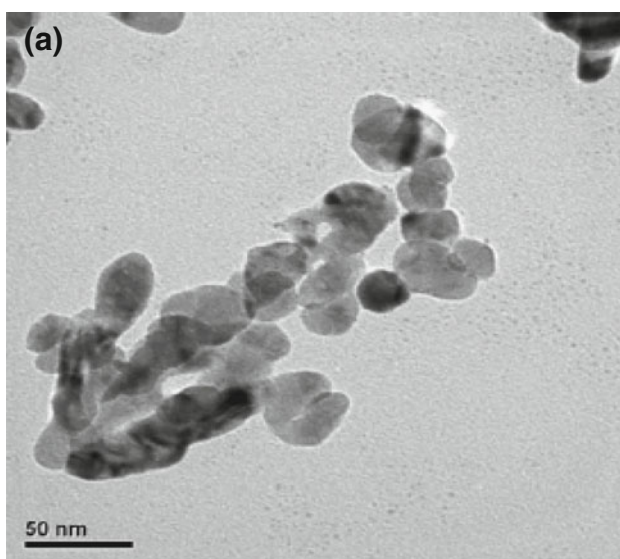
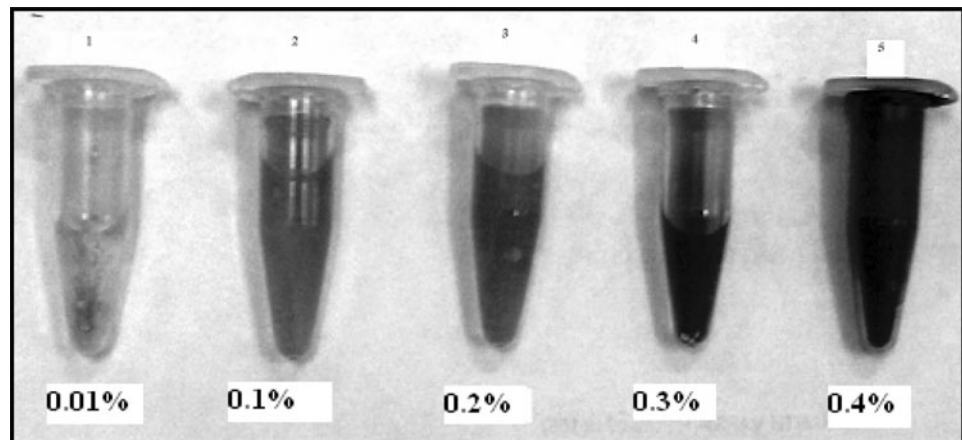
The CuO nanoparticles manufactured by NaBond Technologies Corporation Limited were procured to prepare nanofluids by the two-step method; dispersing dry nanoparticles into the base liquid (distilled water) followed by homogenization. The analysis according to NaBond company standard, the CuO has the following properties as given in the Table 1 below.

Table 1 Analytical result of CuO

Items	Results
Content of CuO	$\geq 99\%$
Average particle size	50 nm
Specific surface area	80 m ² /g

Since the characteristics of nanofluids are governed by not only the kind and size of the nanoparticles but also their dispersion status in the base fluid, it is essential to have the test fluid sample without any agglomeration. To ensure no agglomeration, the nanofluid was stirred in a high speed homogenizer for about 3 h. The test fluid sample was collected in a glass vessel and left for 1 h to verify any agglomeration of the particle and subsequent settling in the vessel bottom. Figure 1 shows the photograph of the test samples at different volumetric compositions with

Fig. 1 CuO Nanofluid in different concentrations. Agglomeration can be observed in sample 1 which was taken before homogenization



negligible agglomeration in the first 60 min. Considering the duration of the test run which is roughly 5 min, no agglomeration for the first 60 min was more than enough to get reliable results from the experimentation.

Figure 2 shows the TEM image of nanoparticles dispersed in distilled water. The TEM image taken showed that the CuO nanoparticles were spheres with a mean diameter of 50 nm and a range from 10 to 100 nm, as given by the manufacturer.

As the flow phenomenon of a liquid–solid solution depends on the hydrodynamic force acting upon the surface of solid particles, volume fraction of the solution is considered to be more important factor as compared to mass fraction. The volume fraction of the fluid is calculated using the following relation.

$$\varphi_v = \frac{1}{\left(\frac{1-\varphi_m}{\varphi_m}\right) \frac{\rho_s}{\rho_l} + 1} \quad (2)$$

Fig. 2 Characteristics of nano-fluid: **a** TEM photograph of CuO nano-particles, **b** size distribution of the nano-particles

Table 2 Major properties of nano-fluids

CuO % φ_v	Density (ρ) _{nf}	Specific heat (C_p) _{nf}	Ratio (C_p) _{nf} / $(C_p)_f$	Brinkman μ_{nf}/μ_l	Drew and Passman μ_{nf}/μ_l	Wasp k_{nf}/k_l
0.01	997.6503	4,176.433	0.997714	1.00025	1.00025	1.000274
0.05	999.8515	4,166.964	0.995453	1.001251	1.00125	1.001372
0.1	1,002.603	4,155.187	0.992639	1.002504	1.0025	1.002746
0.2	1,008.106	4,131.826	0.987058	1.005018	1.005	1.005497
0.3	1,013.609	4,108.718	0.981538	1.00754	1.0075	1.008252
0.4	1,019.112	4,085.86	0.976077	1.01007	1.01	1.011013
0.5	1,024.615	4,063.247	0.970675	1.01261	1.0125	1.013779

where φ_m is the mass concentration of nanoparticles, ρ_l is the liquid density, and ρ_s is the nanoparticle density. Seven different volume concentrations were prepared ranging from 0.01 to 0.5% for experimentation.

From the above equation we can determine the density expression for a solution of liquid–solid as follows.

$$\rho_{nf} = \rho_l(1 - \varphi_v) + \rho_s\varphi_v. \quad (3)$$

The heat capacity of the nanofluid can be determined using the following relation.

$$\rho_{nf}C_{pnf} = \rho_lC_{pl}(1 - \varphi_v) + \rho_sC_{ps}\varphi_v. \quad (4)$$

In a fluid, viscosity and surface tension are also considered important properties. Das et al. have performed a rheological study on alumina nano-fluids. With increasing particle volume fraction, viscosity displayed higher values than that of water. Also, the following equation may be applied in the prediction of viscosity of nanofluids [9].

$$\mu_{nf} = \mu_l(1 + 2.5\varphi_v) \quad (5)$$

The viscosity of the nanofluids can also be estimated by using the equation suggested by Brinkman [10]. Surface tension has only changed slightly in their results. Therefore, the change of the properties of water should have a negligible effect on the present heat transfer results.

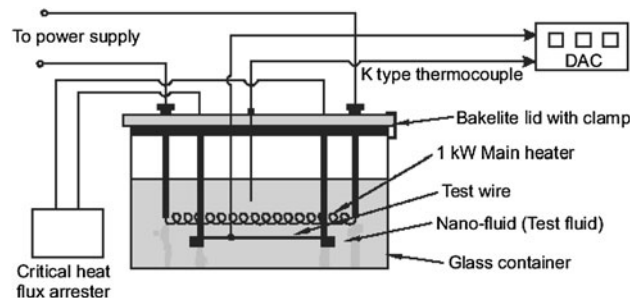
The effective thermal conductivity of solid-liquid mixtures proposed by Wasp [11] is calculated using the following relation.

$$\frac{k_{nf}}{k_l} = \frac{k_s + 2k_l - 2\varphi_v(k_l - k_s)}{k_s + 2k_l + \varphi_v(k_l - k_s)} \quad (6)$$

The thermal conductivity of the solution can be easily calculated through a simplified Hamilton and Crosser model without considering the temperature effect of Das et al. [12] as the following equation.

$$\left(\frac{k_{nf}}{k_l}\right) \approx 1 + \eta_l\varphi_v \quad (7)$$

The thermal conductivity enhancement is a very important physical property of nanofluids as a cooling fluid. However, the volume concentrations in the present

**Fig. 3** Experimental set up

work were too low to expect a considerable enhancement of thermal conductivity. Due to the same reason, the viscosity and density also had nominal changes [13]. The major properties of CuO nanofluid are tabulated in the following Table 2.

2.2 CHF experiments with NiCr wire

Figure 3 shows the experimental set up used for testing CHF of CuO nanofluid. The CHF of de ionized (pure) water and CuO nanofluids was measured with a NiCr wire heater of 36 SWG (0.19 mm diameter), horizontally submerged in the test fluid at atmospheric pressure of 101 kPa. The main test pool consists of a 300 mm diameter, 150 mm high Pyrex glass vessel and a 30 mm thick Bakelite cover. The simple geometry and glass material of the test chamber ensured clean conditions that could be maintained for each experiment. The working fluid is pre-heated using a 1 kW heating coil wound around a metallic strip of tungsten material. The pool temperature is measured with a RTD thermocouple of K-type. Provision is made at the top of the Bakelite cover plate (10 mm diameter hole) to insert the thermocouple lead wire into the boiling liquid. The cover plate can be secured firmly on to the glass vessel containing nanofluid. The hole on the cover ensures atmospheric conditions inside the vessel.

The loss due to evaporation and liquid leakage from the plate was estimated to be 1.33%. This loss was compensated by adding the makeup fluid before the next run. Due

to this, the volume concentration of the working fluid did not change during the pool boiling. A horizontally suspended smooth NiCr wire (test wire) of 0.19 mm diameter was used as testing surface. Both ends of the NiCr wire heater were tightly secured to the clamps of the tungsten electrodes. The heat input to the test wire was measured by a digital Watt meter incorporated for this purpose. After filling the nanofluid into the vessel, it was preheated to saturation temperature using a 1 kW pre-heater. During the experimentation it was observed that the saturation temperature of the nanofluid was about 1–2°C lower as compared to that of pure water due to the addition of nanoparticles. In order to compare the boiling heat transfer among water and nanofluids, the saturated temperatures of pure water (100°C) was taken as the uniform standard. Once the saturation temperature of nanofluid was stabilized, the pre-heater was switched off and the electric power supply to the NiCr wire was switched on. The experiment was conducted by increasing the electric power supply to the wire (test wire). The electric power was increased slowly in small steps using a Variac. For each incremental step, the voltage and corresponding current were recorded in the data acquisition system. As electric power supply to the test wire continued, due to increased electrical resistance of the wire heater, at one particular power input, the test heater burns and breaks instantaneously. Corresponding power input just before the burn out point was recorded by a critical heat input arrester with “peak heat input value” locking arrangement. This maximum electrical power input recorded by the critical heat input arrester was used to calculate critical or burn out heat flux (CHF). The voltage and electric current supplied to the NiCr heating wire heater are used to compute the heat flux as:

$$q = \frac{VI}{A} \tag{8}$$

The main sources of uncertainty of the applied voltage and current are due to contact resistance between the wire heater and electrodes which are connected with only mechanical clamps. In addition, there is uncertainty associated with the length and diameter of the NiCr wire heater. The experimental uncertainty mainly including the parameters like applied voltage and length of the wire is calculated using the following relation proposed by Holman [14] as follows.

If q_{CHF} is a given function of independent variables maximum voltage V_{max} , maximum current I_{max} , diameter of the wire D and length of the wire L , then we have,

$$q_{CHF} = q_{CHF}(V_{max}, I_{max}, D, L)$$

If $U_{q_{CHF}}$ is the uncertainty in the result and $U_{V_{max}}$, $U_{I_{max}}$, U_D and U_L be the uncertainties in the independent

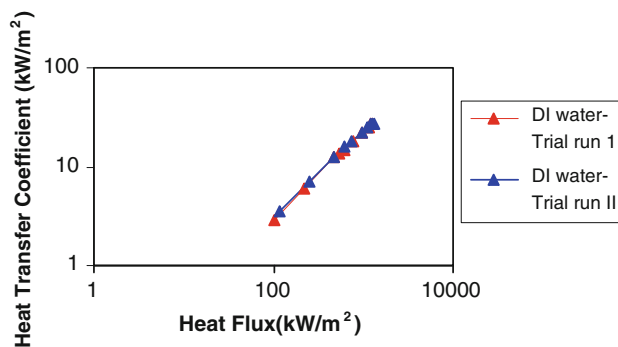


Fig. 4 Experimental repeatability

variables, then uncertainty in the measurement of q_{CHF} having same odds as that in the independent variables, we can write

$$U_{q_{CHF}} = \left[\left(\frac{\partial q_{CHF}}{\partial V_{max}} V_{max} \right)^2 + \left(\frac{\partial q_{CHF}}{\partial I_{max}} I_{max} \right)^2 + \left(\frac{\partial U_{CHF}}{\partial D} D \right)^2 + \left(\frac{\partial q_{CHF}}{\partial L} L \right)^2 \right]^{1/2} \tag{9}$$

Simplifying the above equation we will get

$$U_{q_{CHF}} = q_{CHF} \left\{ \left(\frac{U_{V_{max}}}{V_{max}} \right)^2 + \left(\frac{U_{I_{max}}}{I_{max}} \right)^2 + \left(\frac{U_D}{D} \right)^2 + \left(\frac{U_L}{L} \right)^2 \right\}^{1/2} \tag{10}$$

The uncertainties in the applied voltage, current length and diameter of wire heater are 3.96, 5, 0.7 and 0.526%, respectively. From the above analysis, the maximum uncertainty for pool boiling CHF was estimated to be 4.726%. The accuracy of the thermocouples was confirmed by an ice-bath test with a tolerance of +0.996. Testing of error in Wattmeter was measured with controlled voltage and current source with resistive load using calibrated voltmeter and ammeter. The tolerance reported was –0.326. The experimental repeatability was tested with two trial runs using DI water, the first and second runs yielding CHF of 1.28 and 1.32 MW/m² as shown in Fig. 4.

3 Results and discussion

Figure 5 shows the pool boiling curve of CuO nanofluid till the critical heat flux for two chosen volume concentrations of 0.1 and 0.01% along with DI water. For the other five concentrations similar pattern was observed but with different values of critical heat flux. The steep rise in the heat flux at higher degree of superheat clearly indicates nucleate

Fig. 5 Boiling curve for two volume concentrations of CuO nanofluid

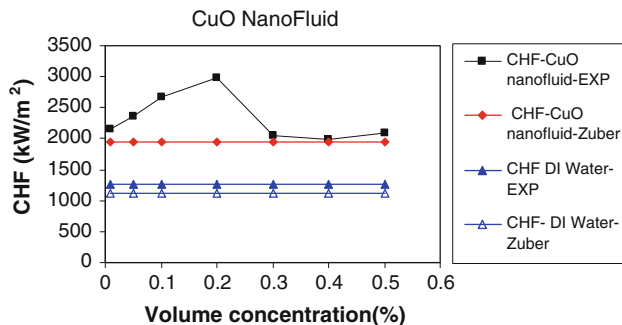
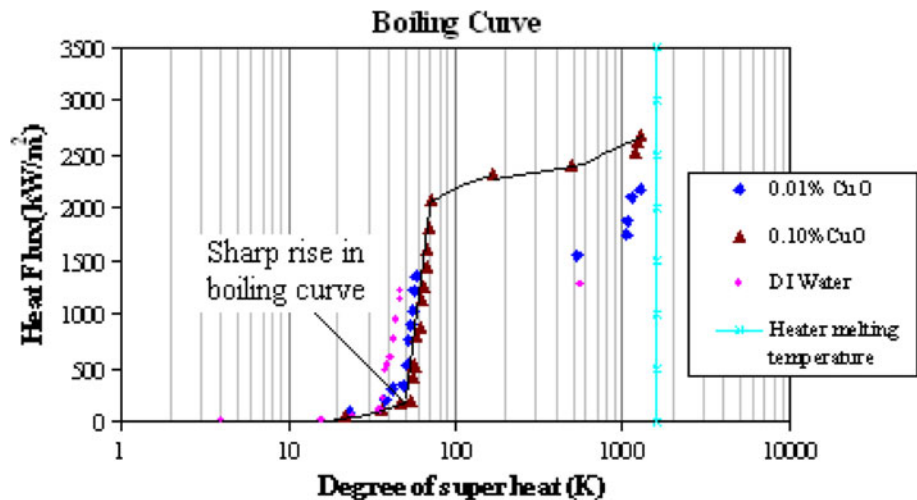


Fig. 6 Variation of CHF with different volume concentrations of CuO nanofluid

pool boiling regime and subsequent sharp rise in curve reaching the burnout point. At 0.01% concentration, CHF increases drastically when compared with water. This indicates even adding extremely small amount of nanoparticles can affect the boiling heat transfer. Further increase in volume concentrations of nanofluid (0.1%), results in shifting of boiling curve to the right. Since the range of the excess temperature in the natural convection regime of nanofluid is wider than that of pure water, the onset of nucleate boiling is delayed and the surface temperature is higher.

Figure 6 shows the measured CHF values of CuO nanofluid at different volume concentrations. Along side corresponding CHF values calculated by using Zuber's equation are also given for comparison purpose. The deviation in CHF from the experimental values using CuO nanofluid is much higher even at lower concentrations when compared to CHF of distilled water obtained by Zuber's equation and experimental method. This behavior is similar to the many earlier observations made by various researchers in the available literatures. The higher value of

CHF and subsequent fall in its value clearly suggests some phenomenon is happening during pool boiling.

It can be noticed from above figure that deviations from the Zuber's correlation using the properties of CuO nanofluid are also very insignificant for CuO concentrations lower than 0.05%, but it has more or less the same magnitude with higher concentrations of nanofluid suggesting that Zuber's equation can be effectively applied to calculate the CHF of nanofluids, but with a modified value of constant on the right hand side of Eq. 1 above. The variation in CHF of nanofluid may be attributed to the formation of porous layer over the test heater surface subsequently making way to deposition of nanoparticles and hence smoothing the surface. The drop in CHF at a higher concentration followed by more or less a constant value as shown in Fig. 6 means, after some optimum thickness of coating over the heater surface, the surface wettability [15] would have reached its maximum value resulting in no further rise in CHF. The present experimental study suggests 0.2% by volume as the optimum value. Nanoparticle depositions also inhibit heat transfer resulting in deterioration of nucleate boiling once this critical value is surpassed. This is in accordance with the observations made by Das et al. Significant CHF enhancement is observed for all concentrations of nanofluid, up to 130% at 0.2% volume concentration. The CHF dependence on nanoparticle concentration is erratic, but not unprecedented for nanofluids.

Figure 7 shows pool boiling CHFs of water- CuO nanofluids with different particle volume concentrations at atmospheric pressure of 101 kPa when compared with pure water. It is clear from Fig. 7 that CuO nanofluids CHF ability is 2.25 times greater than that of water even used in small concentration. In terms of CHF enhancement by the usage of nano-fluids instead of pure water as a

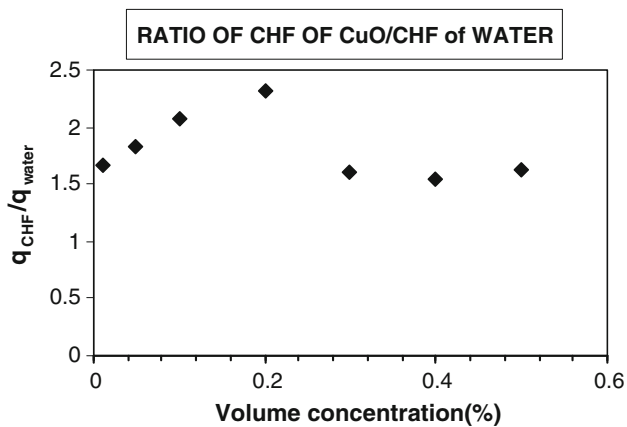


Fig. 7 Ratio of CHF of CuO to CHF of DI water

cooling liquid, the results of the present study are consistent with those of other's works under atmospheric pressure.

Out of several reasons like surface wettability, surface roughness, structural disjoining pressure and capillary wicking responsible for CHF enhancement, this study mainly concentrates on effect of surface roughness on pool boiling. The change in surface roughness was studied under the following two conditions.

3.1 Change in surface roughness when the test surface is exposed to multiple heating cycles

To understand the effect of surface roughness with multiple heating cycles/with aging of wire, test was conducted by mounting the test wire with a constant volume concentration of 0.4% nanofluid. Heat input was slowly increased using the variac. Care was taken not to reach the critical value (all readings taken at 90 W) and the same boiling condition was maintained for 3 min. The sample wire was carefully removed and surface roughness (Ra Value) was measured using "Mitutoyo surftest". In the second run under the same prevailing conditions test wire was exposed to two heating cycles of 3 min duration each and subsequently the surface roughness was measured as explained above. Same procedure was repeated for the third time exposing the test wire to three heating cycles. The result from the above method can be reliable as the test wire was taken from the same lot every time. The following Table 3 shows change in surface roughness with heating cycles at 0.4% volume concentration of CuO nanofluid. The surface roughness measurement in the above test indicated increase in surface roughness of the wire surface.

From the above Table 3 it can be observed that surface roughness value is lower for the first two heating cycles

Table 3 Change in surface roughness with heating cycles at 0.4% volume concentration of CuO nanofluid

Heating cycles (HC)	Bare surface (0-HC) (μm)	1-HC (μm)	2-HC (μm)	3-HC (μm)
Surface roughness (Ra)	0.34	0.23	0.33	0.48

Variation of CHF of CuO nanofluid (0.4% by volume) at different heating cycles/Surface roughness

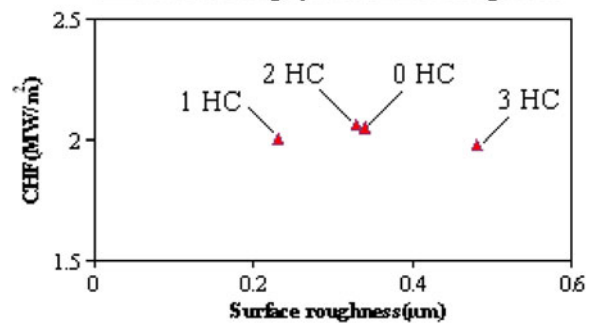


Fig. 8 Variation of CHF value with surface roughness at 0.4% volume concentration of CuO nanofluid at different heating cycles

when compared to the bare heater surface, but it increased when exposed to the third heating cycle. As reported by earlier studies [2, 15], due to decreased surface roughness the wire surface will have lesser nucleation sites resulting in lower value of CHF. This drop in CHF can be seen in the following Fig. 8.

Scanning Electron Microscope (SEM) analysis of the wire surface revealed that the surface is clean during pure water boiling (Fig. 9), but a layer of CuO coating builds up over the wire surface during nanofluid boiling (Figs. 10, 11 and 12). The images are taken for the test wire exposed to multiple heating cycles with 0.4% by volume of CuO nanofluids.

3.2 Change in surface roughness when the test surface is exposed to different volume concentrations of nanofluids

Figure 13b shows the change in surface roughness when the test surface is exposed to different volume concentrations of CuO nanofluid. The surface roughness again increased with increased volume concentrations of nanofluid. The increase in surface roughness can be attributed to formation of a porous layer as seen in the SEM image, Fig. 13a and subsequent filling of nanoparticles in suspension into the micro cavities, thus smoothing the surface. Further exposure of the surface to suspended nanoparticles resulted in roughening of the surface as no more micro

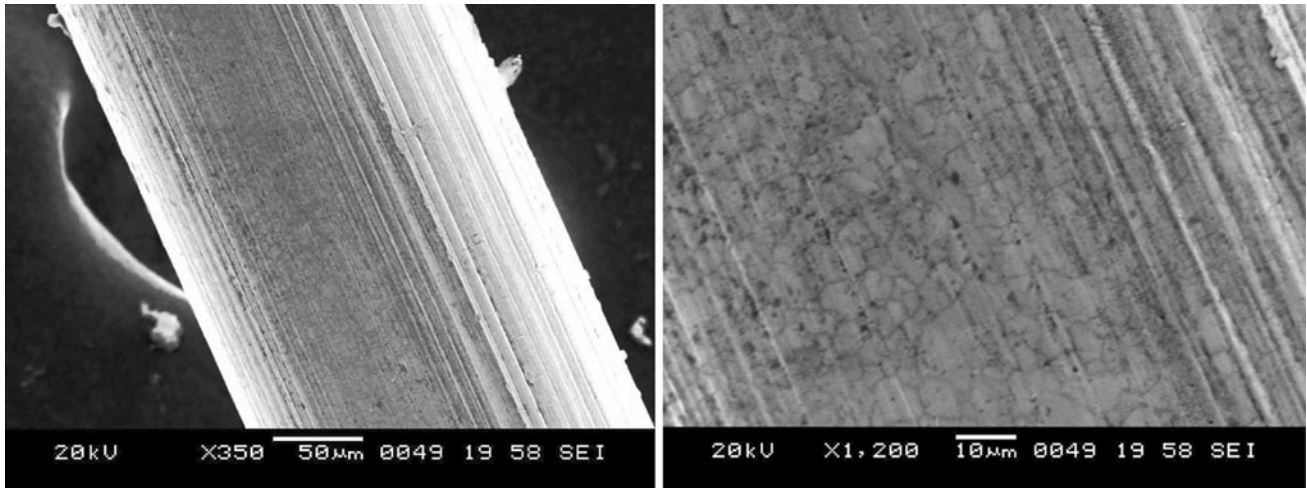


Fig. 9 SEM image of bare heater surface with $\times 350$ and $\times 1,200$ magnification before experiment

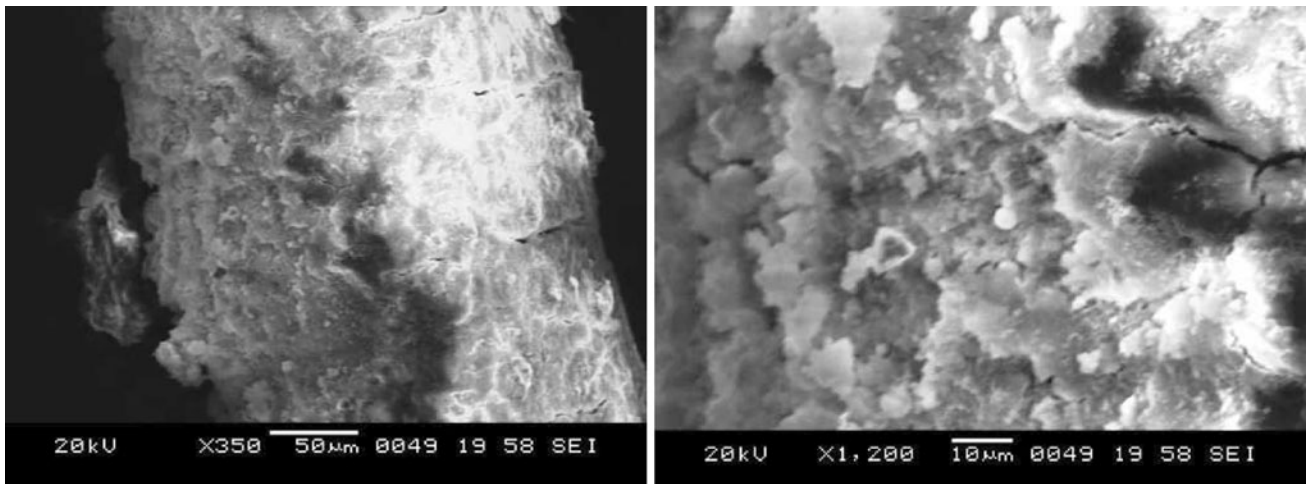


Fig. 10 SEM image of 0.4% CuO nanofluid with $\times 350$ and $\times 1,200$ magnification after exposed to one heating cycle

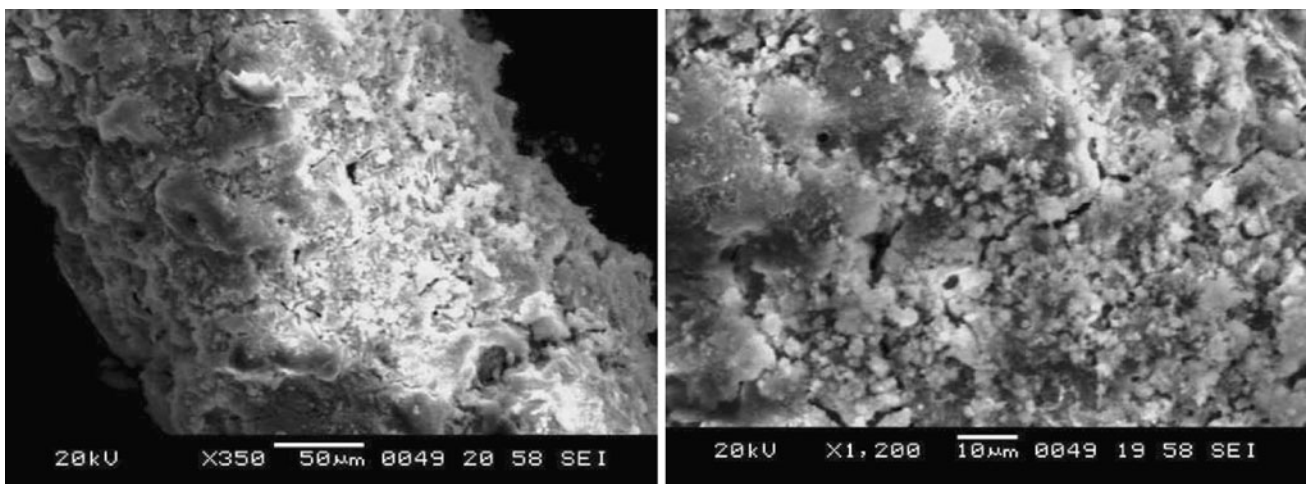


Fig. 11 SEM image of 0.4% CuO nanofluid with $\times 350$ and $\times 1,200$ magnification after exposed to two heating cycles

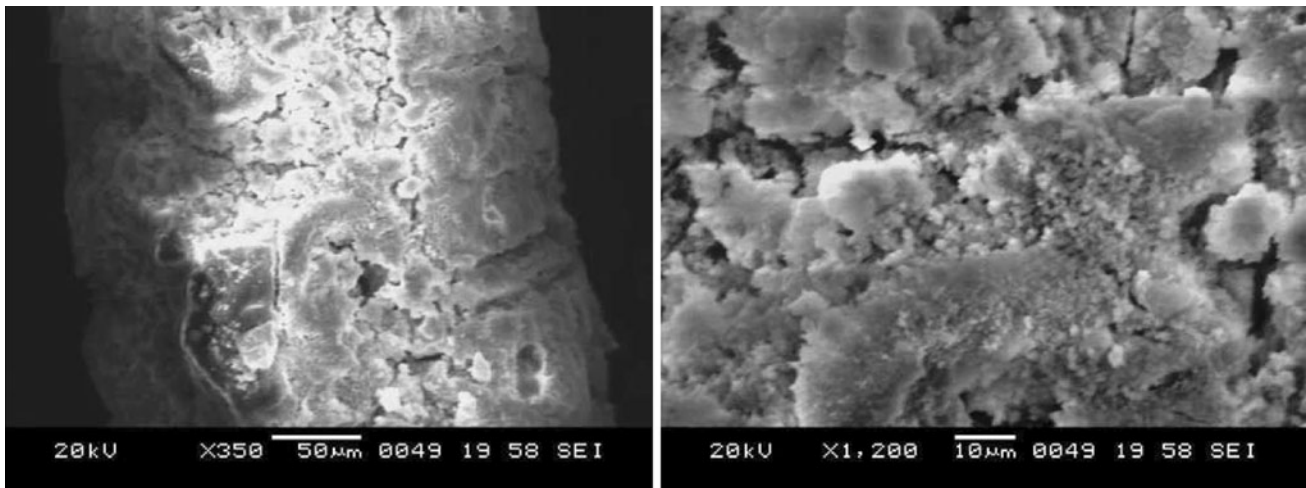


Fig. 12 SEM image of 0.4% CuO nanofluid with $\times 350$ and $\times 1,200$ magnification after exposed to three heating cycles

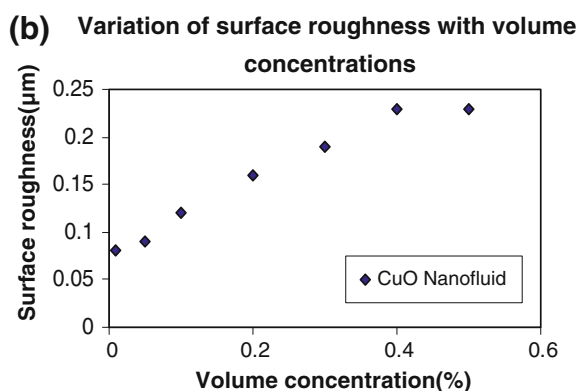
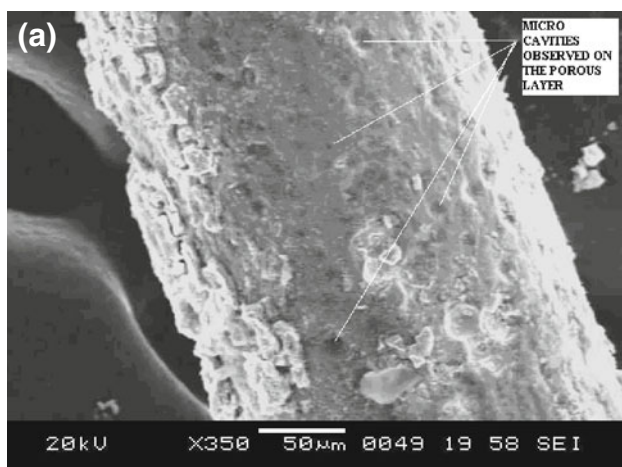


Fig. 13 **a** SEM image showing formation of porous layer with micro cavities. **b** Variation of surface roughness with different volume concentrations of CuO nanofluid

cavities were available. Most probably this layer is formed due to boiling induced precipitation [2] of nanoparticles which was confirmed by surface testing.

Figures 14 and 15 show the SEM images of the test heater surface taken at 0.05% and 0.3% by volume concentrations of CuO nanofluids with $350\times$ and $1,200\times$ magnifications. It can be observed that at 0.3% by volume concentration of CuO nanofluid the surface seems to be smoother compared to 0.05% by volume of CuO nanofluid ($1,200\times$ magnification). The measurement of surface roughness (Ra value) showed roughness of 0.09 and 0.23 μm corresponding to 0.05 and 0.3% volume concentrations of CuO nanofluid. However, it can be observed that even though surface roughness increased (0.3%) while using two volume concentrations (0.05 and 0.3%) it is only relative to the volume concentration and not relative to the surface roughness of fresh heater surface (0.34 μm). This means prolonged exposure of nanofluid to the wire surface can potentially increase the surface roughness of the heater thereby affect boiling heat transfer.

As evident from the above experimental outcome, surface roughness of the heater modified due to increased nanoparticle deposition with respect to time and with respect to volume concentrations. Increase in CHF using nanofluids could be attributed to higher thermal conductivity of nanoparticles coated to the heater surface. However, the variation in CHF could be due to change in surface roughness of the test surface. A smoother surface increased the surface wettability providing more nucleation sites [15] resulting in peak value of CHF (0.2% vol). When the rougher surface formed due to prolonged exposure of nanoparticles during pool boiling, it would have inhibited heat transfer resulting in drop in CHF value. However a detailed study is needed to draw the final conclusion on the optimum thickness of nanoparticle coating which favours peak CHF.

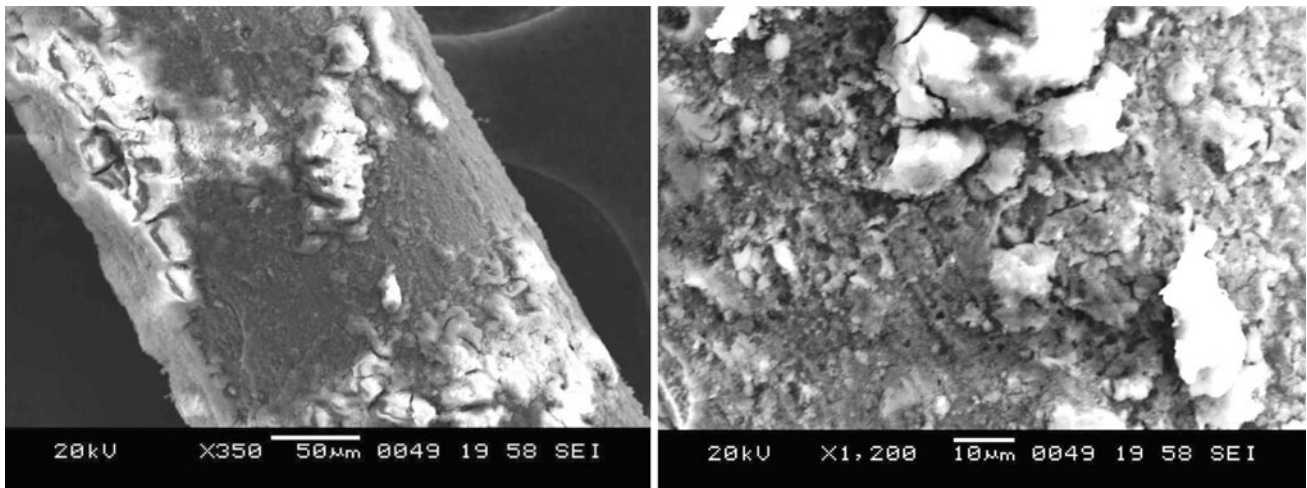


Fig. 14 SEM image of 0.05% CuO nanofluid with $\times 350$ and $\times 1,200$ magnification after exposed to three heating cycles

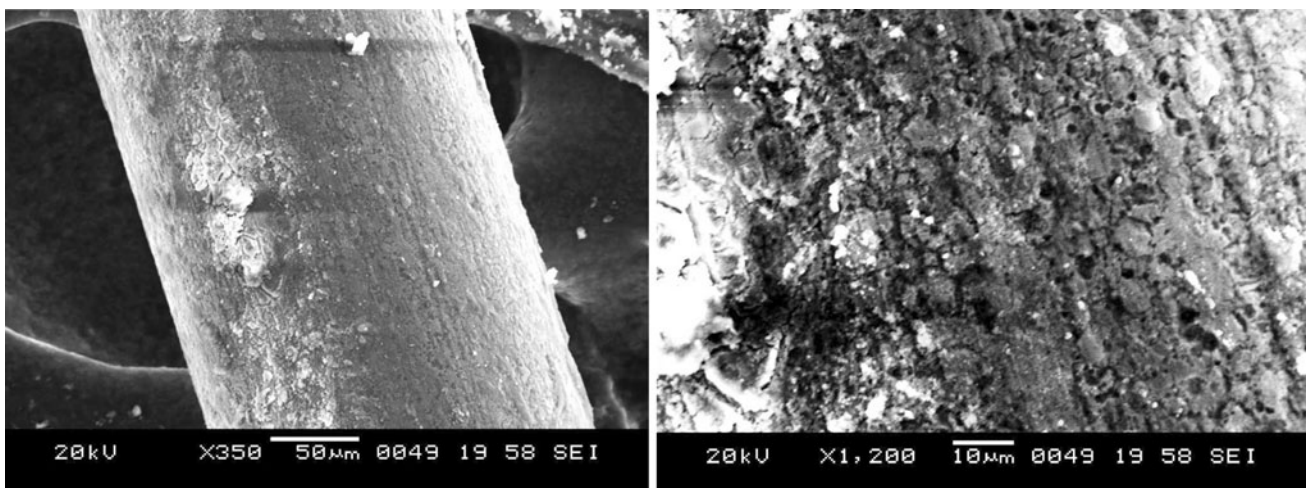


Fig. 15 SEM image of 0.3% CuO nanofluid with $\times 350$ and $\times 1,200$ magnification after exposed to three heating cycles

4 Conclusions

Pool boiling CHF characteristics of nano-fluids were investigated with seven volume concentrations of CuO nanofluid ranging from 0.01 to 0.5%, and the effect of surface roughness in pool boiling CHF of CuO nano-fluids for each concentration was studied experimentally.

- During the experimentation, the pool boiling CHF of CuO nanofluids on a bare heater of NiCr wire was enhanced to $\sim 130\%$ compared to that of pure water by increasing nanoparticle concentration. It was observed that with low concentration of CuO the dispersion was homogeneous while higher concentration of CuO resulted in the formation of coating over the heater surface and fouling of the vessel inner surface.
- The surface roughness measurement and the corresponding SEM images of the heater surface taken for two different conditions namely, (1) when the test surface is exposed to multiple heating cycles (2) when the test surface is exposed to different volume concentrations of nanofluids after pool boiling CHF tests, revealed that CHF enhancement of nano-fluids was closely related to the surface microstructure and enhanced topography resulting from the deposition of nanoparticles. The study also revealed that change in surface roughness is not only results from change in concentration of the nanofluid but also with change in time. In both the above cases nanoparticle deposition increases resulting in decreased surface roughness.
- The CHF value reached a maximum and then remained constant in magnitude suggesting thickness of

deposition matters in deciding the CHF which in turn can affect boiling heat transfer.

References

1. You SM, Kim J, Kim KH (2003) Effect of nanoparticles on critical heat flux of water in pool boiling heat transfer. *Appl Phys Lett* 83:3374–3376
2. Das S, Putra N, Roetzel W (2003) Pool boiling characteristics of nanofluids. *Int J Heat Mass Transf* 46:851–862
3. Vassallo P, Kumar R, Amico SD (2004) Pool boiling heat transfer experiments in silica-water nanofluids. *Int J Heat Mass Transf* 47:407–411
4. Bang IC, Chang SH (2005) Boiling heat transfer performance and phenomena of Al_2O_3 -water nanofluids from a plain surface in a pool. *Int J Heat Mass Transf* 48:2407–2419
5. Wen D (2008) Mechanisms of thermal nanofluids on enhanced critical heat flux (CHF). *Int J Heat Mass Transf* 51:4958–4965
6. Kwark SM, Kumar R, Moreno G, Yoo J, You SM (2010) Pool boiling characteristics of low concentration nanofluids. *Int J Heat Mass Transf* 53:972–981
7. Kutateladze SS (1951) A hydrodynamic theory of changes in the boiling process under free convection conditions. *Izv Akad Nauk USSR Otd Tekh Nauk* 4:529–935
8. Zuber N (1959) Hydrodynamic aspects of boiling heat transfer. AEC Rep AECU 4439
9. Drew DA, Passman SL (1999) *Theory of multicomponent fluids*. Springer, Berlin
10. Brinkman HC (1951) The viscosity of concentrated suspension and solutions. *J Chem Phys* 20:571
11. Wasp FJ (1977) *Solid-liquid slurry pipeline transportation*. Trans Tech, Berlin
12. Das SK, Putra N, Thiesen P, Roetzel W (2003) Temperature dependence of thermal conductivity enhancement for nanofluids. *J Heat Transf Trans ASME* 125:567–574
13. Murshed SMS, Leong KC, Yang C (2005) Enhanced thermal conductivity of TiO_2 -water based nanofluids. *Int J Thermal Sci* 44:367–373
14. Holman JP (2007) *Experimental methods for engineers*, 7th edn. McGraw-Hill, New York
15. Kim SJ, Bang IC, Buongiorno J (2007) Surface wettability change during pool boiling of nanofluids and its effect on critical heat flux. *Int J Heat Mass Transf* 50:4105–4116